ELSEVIER

www.elsevier.nl/locate/jorganchem

Journal of Organometallic Chemistry 589 (1999) 85–91

Journal of Organometallic Chemistry

Linear free-energy relationships and inverted Marcus region in the horseradish peroxidase-catalyzed oxidation of ferrocenes by hydrogen peroxide

Alexander D. Ryabov [a,b,*], Vasily N. Goral [a], Ekaterina V. Ivanova [a], Marina D. Reshetova [a], Andreas Hradsky [c], Benno Bildstein [c]

[a] *Department of Chemistry, M.V. Lomonosov Moscow State University, 119899, Moscow, Russia*
[b] *Division of Chemistry, G.V. Plekhanov Russian Economic Academy, Stremyanny per. 28, 113054, Moscow, Russia*
[c] *Institut für Allgemeine, Anorganische und Theoretische Chemie, Universität Innsbruck, Innrain 52a, A-6020 Innsbruck, Austria*

Received 23 February 1999

Abstract

Second-order rate constants (k_3) for the steady-state horseradish peroxidase (HRP, isoenzyme C)-catalyzed oxidation of a variety of mono-, di (1,1′)-, and pentamethyl ferrocenes by hydrogen peroxide into the corresponding ferricenium cations at 25°C, pH 7 have been used to investigate steric and electronic effects on the reactivity in terms of the linear free-energy relationships (LFER) and the Marcus formalism for an outer-sphere electron transfer. There is a linear correlation with a negative slope between $\ln k_3$ and the formal redox potentials of ferrocenes ($E°'$) for the mono- and di-substituted molecules suggesting that, in this series, k_3 increases with increasing the reaction driving force. The pentamethylated derivatives $Cp^*FeC_5H_4X$, the $E°'$ values of which are significantly lower compared with other ferrocenes, display markedly lower reactivity as to be anticipated based on LFER. This observation is rationalized by assuming that the great increase in the driving force for $Cp^*FeC_5H_4X$ is neutralized by the steric retardation imposed by the pentamethlyated cyclopentadienyl ring. The steric hindrance is believed to increase in the electron transfer distance from the organometallic donor to the heme of HRP which takes place on going from $C_5H_4YFeC_5H_4X$ to $Cp^*FeC_5H_4X$ species. Alternatively, the reactivity trends reported can be accounted for in terms of the Marcus theory for the outer-sphere electron transfer, the $Cp^*FeC_5H_4X$ species being the spectators of the inverted Marcus region.

Keywords: Horseradish peroxidase; Ferrocenes; Oxidation; Linear free-energy relationship; Marcus theory

1. Introduction

One major task of the nowadays rapidly developing area referred to as organometallic biochemistry or bioorganometallic chemistry [1–3] is elucidating the factors that determine the reactivity of organometallic compounds toward enzymes. The main interest here is dictated by the fact that the overwhelming majority of organometallic molecules are unnatural substrates of enzymes which, in addition, often provide unnatural chirality types, and, therefore, there is a challenge to force these molecules to be accepted and rapidly transformed by biocatalysts. Our recent interests have been aimed at various aspects of oxidation of ferrocenes by hydrogen peroxide catalyzed by horseradish peroxidase (HRP) into the corresponding ferricenium ions. This enzyme has recently became an object of intensive study [4,5] including X-ray structural determinations [6,7]. We first studied the stoichiometry of the oxidation and demonstrated that the procedure can be used for routine one-pot monitoring of the amount of H_2O_2 in samples [8]. The kinetic study under steady state revealed that the oxidation follows first-order kinetics both in ferrocenes and HRP, ferrocene proving to be a reactive substrate of the enzyme [9]. A stopped-flow investigation has demonstrated that it is the electron transfer from ferrocenes at HRP Compound II that is

* Corresponding author. Fax: +7-95-9395417.
E-mail address: adr@enzyme.chem.msu.ru (A.D. Ryabov)

0022-328X/99/$ - see front matter
PII: S0022-328X(99)00321-6

the rate-limiting step under the steady state [10]. We learned that HPR is capable of chiral discrimination between the planar chiral enantiomers of (*R*)- and (*S*)-2-methylferrocene carboxylic acid [11], whereas the covalent coupling of ferrocene with typical organic substrates of HRP, such as aniline and phenol, affords HRP substrates the reactivity of which exceeds 100-fold that of the corresponding precursors [12]. It has recently been shown that the conjugate derived from aminomethylferrocene and hemin can be incorporated into apo-HRP to produce the electrochemically and catalytically active biocatalyst with altered substrate specificity [13]. All our previous findings suggest that the HRP-promoted oxidation of ferrocenes depends both on their formal redox potentials ($E°'$) and steric features. In order to obtain a more clear picture of the contribution of the two effects to the reactivity, we have investigated the steady-state kinetics of the oxidation of a variety of mono-, di- (1,1′), and polysubstituted ferrocenes (Chart 1), as well as measured the $E°'$ values under the same conditions. The analysis of the kinetic data obtained in this work and elsewhere [9,10] in terms of free-energy correlations indicates that, unfortunately, it is impossible to increase the reactivity of ferrocenes by their extensive methylation which results in a dramatic decrease in the formal redox potentials. The reasons for that are discussed in this work together with an alternative rationalization of the kinetic data in terms of the Marcus electron-transfer formalism [14,15].

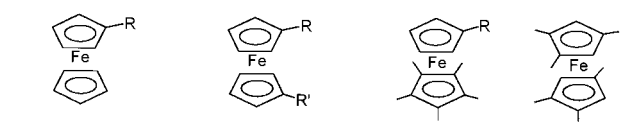

R = H (**1**)
Me (**2**)
Et (**3**)
n-Bu (**4**)
CO_2H (**5**)
CH_2CO_2H (**6**)
CH_2NMe_2 (**7**)
$CO(CH_2)_2CO_2H$ (**8**)
$CO(CH_2)_3CO_2H$ (**9**)
CHOHMe (**10**)
C(Me)=NOH (**11**)

R = R' = CO_2H (**12**)
R = Et, R' = $CO(CH_2)_2CO_2H$ (**13**)
R = n-Bu, R' = CO_2H (**14**)

R = H (**15**)
CO_2H (**16**)
CH_2NMe_2 (**17**)

(**18**)

(Chart 1)

2. Results

2.1. Formal kinetics

As known [8], the HRP-catalyzed oxidation of ferrocenes by H_2O_2, which was first reported in this journal more than two decades ago [16], follows Eq. (1):

$$2RFc + H_2O_2 + 2H^+ \overset{HRP}{\rightarrow} 2RFc^+ + 2H_2O \quad (1)$$

and it is easy follow the steady-state kinetics of reaction (1) by monitoring the formation of the ferricenium cations at ca 630 nm [9]. The extinction coefficients for reaction products required for such a procedure were evaluated as described before [8]. As in the previous work [9], where this issue was discussed in much detail, all ferrocenes listed in Chart 1 display first-order kinetics both in RFc and HRP. The data shown in Fig. 1 for the example of $Cp^*FeC_5H_4COOH$ (**16**) are an illustration of the former, less common for enzymatic reactions, phenomenon. As expected, a first order in HRP holds at concentrations up to 10^{-7} M. The measurements were made at the optimal concentration of H_2O_2 (2.4×10^{-4} M) around which the rate of reaction (1) is independent of $[H_2O_2]$ [9].

The major problem encountered in these studies is a low solubility of ferrocene derivatives bearing no polar or charged functional groups. The solubility is however enhanced in the presence of micelles of surfactants such as Triton X-100, for example. Since the rate of enzymatic reaction is known to be strongly affected by the surfactant [9], the reaction rate was measured at different concentrations of Triton X-100 and the data were extrapolated to zero surfactant concentration using Eq. (2) [9,17,18]:

$$k_{obs} = \frac{k_w}{1 + PCV} \quad (2)$$

where k_{obs} is the second-order rate constant for the interaction between HRP and RFc in the presence of hydrogen peroxide; k_w is the corresponding rate constant referring to the aqueous phase (which should be associated with k_3, see below); P is the partition coefficient for RFc between the micellar and aqueous pseudo-phase; C is the surfactant concentration without critical micelle concentration (cmc), V is the molar volume of micelles.

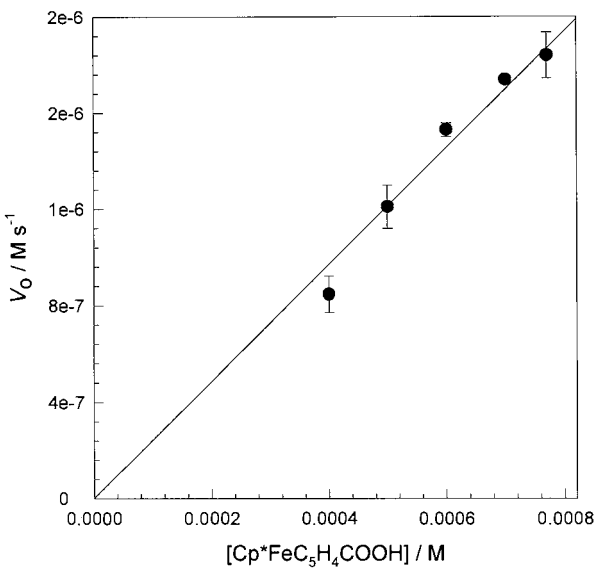

Fig. 1. Steady-state rate of HRP-catalyzed oxidation of $Cp^*FeC_5H_4COOH$ (**16**) by H_2O_2 as a function of [**16**]; $[H_2O_2]$, 2×10^{-4} M; [HRP], 10^{-7} M, pH 7.0, 25°C.

Table 1
Observed second-order rate constants for HRP-catalyzed oxidation of water-insoluble ferrocenes by H_2O_2 at different Triton X-100 concentrations at pH 7, 25°C

No.	Ferrocene derivative	[Triton X-100] (M)	k_{obs} (M^{-1} s^{-1})
6	$FcCH_2CO_2H$	0.005	$(4.27 \pm 0.08) \times 10^4$
		0.01	$(3.66 \pm 0.06) \times 10^4$
		0.02	$(3.26 \pm 0.08) \times 10^4$
		0.03	$(2.6 \pm 0.2) \times 10^4$
		0.04	$(2.5 \pm 0.1) \times 10^4$
		0.05	$(2.25 \pm 0.05) \times 10^4$
10	FcCHOHMe	0.005	$(9.8 \pm 0.1) \times 10^3$
		0.01	$(7.58 \pm 0.09) \times 10^3$
		0.02	$(6.12 \pm 0.03) \times 10^3$
		0.03	$(4.6 \pm 0.1) \times 10^3$
		0.04	$(3.6 \pm 0.4) \times 10^3$
		0.05	$(3.6 \pm 0.2) \times 10^3$
11	FcC(Me) = NOH	0.01	$(2.8 \pm 0.1) \times 10^4$
		0.02	$(2.4 \pm 0.1) \times 10^4$
		0.03	$(2.1 \pm 0.1) \times 10^3$
		0.04	$(1.3 \pm 0.1) \times 10^3$
		0.05	$(1.3 \pm 0.2) \times 10^3$
8	$FcCO(CH_2)_3CO_2H$	0.005	$(9.51 \pm 0.05) \times 10^2$
		0.01	$(7.58 \pm 0.02) \times 10^2$
		0.03	$(6.14 \pm 0.06) \times 10^2$
		0.04	$(4.80 \pm 0.02) \times 10^2$
		0.05	$(5.16 \pm 0.06) \times 10^2$
15	Cp*FeCp	0.005	$(4.6 \pm 0.2) \times 10^3$
		0.01	$(2.98 \pm 0.08) \times 10^3$
		0.02	$(2.3 \pm 0.1) \times 10^3$
		0.03	$(1.6 \pm 0.1) \times 10^3$
		0.04	$(1.31 \pm 0.07) \times 10^3$
		0.05	$(8.65 \pm 0.01) \times 10^2$
17	$Cp^*FeC_5H_4CH_2NMe_2$	0.005	$(1.3 \pm 0.2) \times 10^3$
		0.01	$(8.0 \pm 0.9) \times 10^2$
		0.02	$(8.0 \pm 0.9) \times 10^2$
		0.03	$(5.8 \pm 0.6) \times 10^2$
		0.04	$(4.5 \pm 0.5) \times 10^2$
		0.05	$(3.7 \pm 0.4) \times 10^2$
18	1,2,4,1′,2′,4′-Me_6Fc	0.015	$(5.6 \pm 0.9) \times 10^3$
		0.02	$(4.5 \pm 0.4) \times 10^3$
		0.025	$(3.3 \pm 0.3) \times 10^3$
		0.03	$(3.6 \pm 0.6) \times 10^3$
		0.04	$(2.5 \pm 0.1) \times 10^3$
		0.05	$(2.2 \pm 0.2) \times 10^3$

The second-order rate constants as a function of Triton X-100 concentration for poorly water-soluble ferrocenes are summarized in Table 1. Table 2 contains the rate constants k_3 obtained either directly in aqueous solution for water-soluble ferrocenes or calculated by extrapolation to zero Triton X-100 concentration according to Eq. (2). The fact that in the latter case the reaction rate drops as the surfactant concentration increases is illustrated by Fig. 2, where the data for 1,2,4,1′,2′,4′-Me_6Fc (**18**) are presented. For comparison, it is shown in Fig. 3 that the reaction rate is [Triton X-100] independent for water-soluble ferrocene such as $Cp^*FeC_5H_4COOH$ (**16**).

2.2. Formal redox potentials

Formal redox potentials of ferrocenes used in this work are summarized in Table 2, which contains the values measured directly in the case of water-soluble species and extrapolated to zero surfactant concentration [19] for insoluble ones, the data being obtained in micellar solutions of Triton X-100. In most of the cases the measured potentials displayed a weak dependence on Triton X-100 concentration.

3. Discussion

3.1. Two groups of ferrocenes in LFER

As it was briefly mentioned in Section 1, the rate-limiting step in the steady-state oxidation of ferrocenes by H_2O_2 catalyzed by HRP is the electron transfer from HRP Compound II [10], which is driven by the rate constant k_3.

$$HRP + H_2O_2 \rightarrow HRP\text{-}I \quad k_1$$

$$HRP\text{-}I + RFc \rightarrow HRP\text{-}II + RFc^+ \quad k_2$$

$$HRP\text{-}II + RFc \rightarrow HRP + RFc^+ \quad k_3$$

Here, HRP-I and HRP-II are the so-called HRP Compounds I and II which are by two and one oxidative equivalents above the resting state of HRP, respectively. Data in Table 2 as $\ln k_3$ against $E^{\circ\prime}$ are presented in Fig. 4. As seen, all ferrocenes studied fall into two (or, strictly speaking, three if unsubstituted ferrocene can be treated as a group) groups. The first one comprises mono- and 1,1′-disubstituted ferrocenes (Group I), whereas the second group consists of $Cp^*FeC_5H_4X$ molecules and 1,2,4,1′,2′,4′-hexamethylferrocene (Group II), the redox potentials of which are shifted cathodically by 200–400 mV compared to Group I ferrocenes. There is a linear dependence between $\ln k_3$ and $E^{\circ\prime}$ (in mV) within each of the two groups and the corresponding linear regressions are given by Eqs. (3) and (4):

$$\ln k_3(\mathrm{I}) = (12.4 \pm 0.6) - (0.010 \pm 0.002)E^{\circ\prime} \quad (3)$$

$$\ln k_3(\mathrm{II}) = (9.8 \pm 0.2) - (0.042 \pm 0.007)E^{\circ\prime} \quad (4)$$

An objective or even the goal of this study was to observe enhanced reactivity in the case of Group II ferrocenes, the reaction driving force for which is significantly higher. This could be the case if Group I and

Table 2
The second-order rate constants for HRP-catalyzed oxidation of substituted ferrocenes by H_2O_2 (2×10^{-4} M) at pH 7, 25°C

No.	Ferrocene derivative	k_3 (M^{-1} s^{-1})	$E^{o\prime}$ (mV) (vs. SCE)	P	Reference
1	FcH	$(1.93\pm0.05)\times10^5$	210 ± 5	460 ± 60	[9]
2	FcMe	$(4.01\pm0.06)\times10^4$ [a]	100	200 ± 30	[9]
3	FcEt	$(2.71\pm0.06)\times10^4$	222 ± 5	250 ± 30	[9]
4	FcBu-*n*	$(5.92\pm0.07)\times10^3$	304 ± 5	390 ± 50	[9]
5	FcCOOH	$(8.90\pm0.06)\times10^3$	290 ± 5		[10]
6	$FcCH_2COOH$	$(4.20\pm0.40)\times10^4$	132 ± 5	120 ± 10	This work
7	$FcCH_2NMe_2$	$(2.44\pm0.08)\times10^3$	345 ± 5		[10]
8	$FcCO(CH_2)_2COOH$	$(9.5\pm0.3)\times10^2$	488 ± 5		This work
9	$FcCO(CH_2)_3COOH$	$(9.2\pm0.2)\times10^2$	552 ± 5	81 ± 7	This work
10	FcCHOHMe	$(1.25\pm0.03)\times10^4$	204 ± 5	150 ± 10	This work
11	FcC(Me)=NOH	$(3.3\pm0.3)\times10^4$	320 ± 5	115 ± 9	This work
12	$1,1'$-$(HOOC)_2Fc$	$(6.7\pm0.4)\times10^3$	382 ± 5		This work
13	1-Et-$1'$-$(CO(CH_2)_2COOH)Fc$	$(1.62\pm0.06)\times10^4$	330 ± 5		This work
14	1-n-Bu-$1'$-HOOCFc	$(5.6\pm0.2)\times10^4$	206 ± 5		This work
15	Cp*FeCp	$(4.4\pm0.4)\times10^3$	35 ± 5	240 ± 20	This work
16	$Cp^*FeC_5H_4COOH$	$(1.25\pm0.04)\times10^4$	5 ± 5		This work
17	$Cp^*FeC_5H_4CH_2NMe_2$	$(2.1\pm0.2)\times10^3$	50 ± 5	109 ± 9	This work
18	$1,2,4,1',2',4'$-Me_6Fc	$(1.1\pm0.1)\times10^4$	17 ± 5	320 ± 60	This work

[a] This value was calculated from $k_{obs}=2\times10^4$ M^{-1} s^{-1} measured at [Triton X-100] = 0.04 M using Eq. (2) and assuming $P\approx200$ and $V\approx0.3$ cm^3 mol^{-1}.

Group II ferrocenes display similar kinetic behavior driven by one and the same linear free-energy relationship (LFER). This, however, did not occur and Group II molecules comprise an independent reaction series.

We have previously emphasized [9] that the key feature of reaction (1) is a first-order kinetics in the substrate indicative of kinetic insignificance of the enzyme–substrate binding. This points to an intermolecular electron transfer from ferrocenes to HRP-II in the rate-limiting step. The fact that the linear free-energy relationship holds for Group I compounds suggests that, within the series, the HRP-catalyzed oxidation of ferrocenes is an electronically driven process with an approximately similar distance of the electron transfer. Introduction of the steric bulk to ferrocenes gives rise to a new set (Group II) without the expected rate increase. There are two possible rationalizations for this effect. The first is based on our previous mechanistic conclusions [9]. It was suggested that the electron transfer has features typical of an outer-sphere process and the ferrocenes approach partly exposed to solution heme edge which is ca. 8–11 Å from the iron (Fig. 5). Fig. 5 was created on the basis of X-ray structural data for horseradish peroxidase isoenzyme C [6] and using a Sculpt 2.6.0. program for optimization of the structures of ferrocene and pentamethylferrocene. Pentamethylated ferrocenes are obviously much bulkier than Group I molecules. Therefore, it is reasonable to assume that bulkier Group II ferrocenes cannot approach the heme edge as closely as Group I molecules (cf. Fig. 5(a) and (b)). In the case of Group II molecules, the electron should overcome longer distance in order to reach the heme edge. Consequently, the increase in the reaction driving force can be neutralized by the unfavorable elongation of the electron-transfer pathway [20]. The latter seems to be the dominating effect in this process bringing about the overall rate decrease.

3.2. Marcus formalism

An alternative rationale of the existence of Groups I and II is based on the Marcus formalism [15]. A similar approach has recently been applied to the kinetics of HRP-catalyzed oxidation of phenols [21,22]. In our case, the data in Fig. 4 can be replotted so as to highlight the inverted Marcus region in reaction 1 (Fig. 6). The following standard assumptions have been made in our calculations [14,15]:

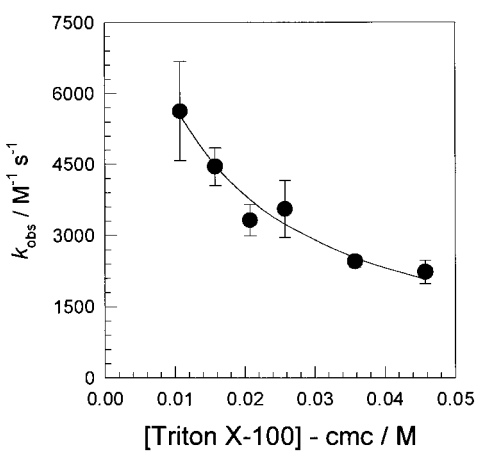

Fig. 2. Steady-state rate of HRP-catalyzed oxidation of $1,2,4,1',2',4'$-hexamethylferrocene (**18**) by H_2O_2 as a function of [Triton X-100]; [H_2O_2], 2×10^{-4} M; [HRP], 10^{-7} M, [**18**], 10^{-3} M, pH 7.0, 25°C.

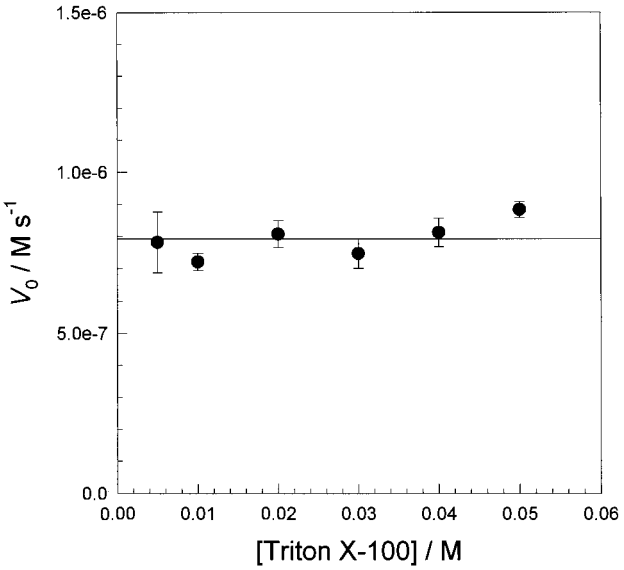

Fig. 3. Steady-state rate of HRP-catalyzed oxidation of Cp*FeC_5H_4COOH by H_2O_2 as a function of [Triton X-100]; [H_2O_2], 2×10^{-4} M; [HRP], 10^{-7} M, [**16**], 10^{-3} M, pH 7.0, 25°C.

$$k_3 = k_{ET}K_{OS}, \qquad k_{ET} = k_0 e^{-\frac{\Delta G^{\neq}}{RT}}$$

$$\Delta G^{\neq} = \frac{\lambda}{4}\left(1 + \frac{\Delta G^{\circ}}{\lambda}\right)^2$$

Here, k_{ET} is the electron-transfer rate constant within an outer-sphere enzyme-substrate intermediate the stability of which is determined by K_{OS}; k_0 is the rate constant for activationless electron transfer; and λ is the reorganization parameter. A combination of these equations results in Eq. (5) on condition that $\Delta G^{\circ} = -nF\Delta E$, F is expressed in eV/V and $E^{\circ\prime} = 0.869$ V for the HRP-II/HRP couple (versus NHE) [23].

$$\log k_3 = \log(k_0K_{OS}) - \frac{\lambda}{4}\left(1 + \frac{\Delta E}{\lambda}\right)^2 \qquad (5)$$

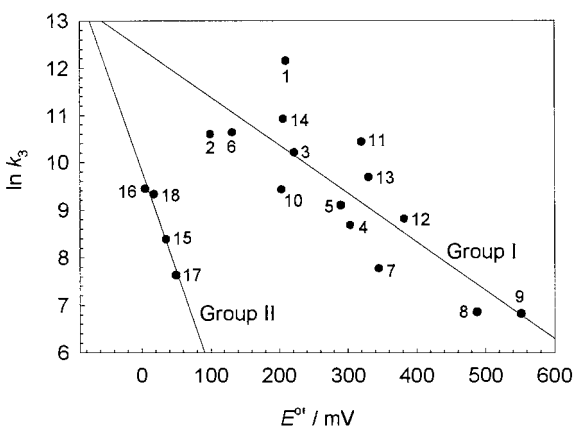

Fig. 4. LFER plot for ln k_3 vs. $E^{\circ\prime}$ using the data from Table 2. Numbers correspond to ferrocenes shown in Chart 1.

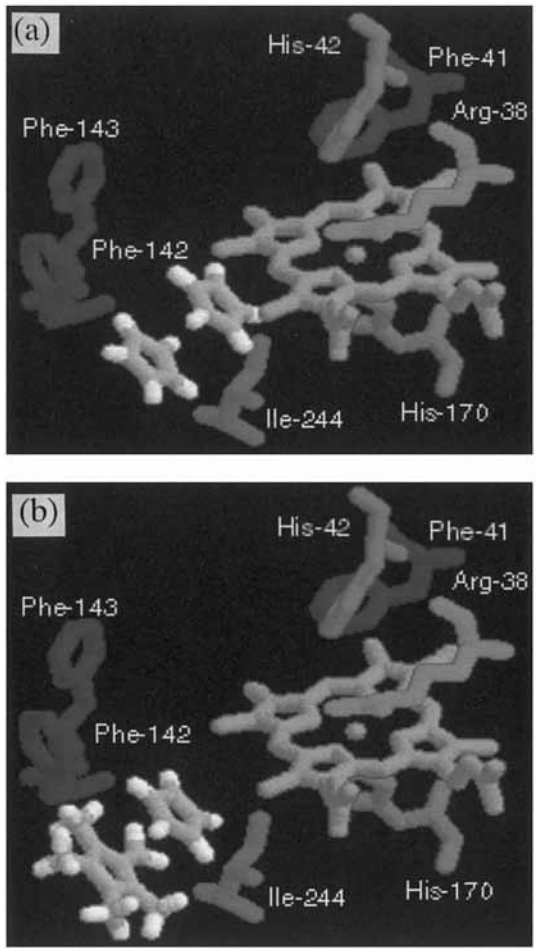

Fig. 5. Graphical visualization of the steric requirements during the approach of ferrocene (a) and pentamethylferrocene (b) to the heme edge of HRP. For details, see text.

The data in Fig. 6 were fitted to Eq. (5), and the best-fit values for (k_0K_{OS}) and the reorganization parameter λ equal $(1.9 \pm 0.4) \times 10^4$ M^{-1} s^{-1} and 0.45 ± 0.04 eV, respectively. The latter is very close to that found in HRP-catalyzed oxidation of phenols [22]. The parabolic dependence appears to be satisfactory in this case. However, we do not intend to overestimate this observation and prefer to regard it as one of the possibilities, since the rationale based on entirely steric reasons resulting in elongation of the electron-transfer distance also seems to be valid. It should only be mentioned that Group II ferrocenes underscore the inverted region, which was not clearly observed in the case of HRP-catalyzed oxidation of phenols [21].

The reactivity of unsubstituted ferrocene deserves a comment. Despite the mechanistic treatment, it is noticeably more reactive compared, for instance, to monosubstituted ferrocenes. This is nicely seen in both Figs. 4 and 6. Again, we assume that the symmetry of the molecule plays a key role here. In contrast to monosubstituted ferrocenes **2**–**11**, unsubstituted ferrocene **1** has

equal possibilities in terms of approaching the heme edge by its two unsubstituted cyclopentadienyl rings (Fig. 5(a)). Obviously, the attack of heme by molecules **2**–**11** will be less advantageous, since the steric repulsion is to be expected when the latter approach heme from the side of the monosubstituted cyclopentadienyl ring. Therefore, at least a two-fold increase in the reactivity should be expected for ferrocene **1** for a purely statistical reason.

In conclusion, we have demonstrated that a dramatic increase of the reaction driving force in the HRP-catalyzed oxidation of ferrocenes by H_2O_2 at the expense of extensive methylation of the cyclopentadienyl rings *does not* bring about the anticipated rate enhancement. Two approaches have been used for the rationalization of the second-order rate constants for the rate-limiting electron transfer from various ferrocene derivatives at HRP Compound II. The first is based on a classical LFER routine that revealed the splitting of the ferrocene family into two groups. The steric bulk is assumed to be responsible for the splitting which, on the molecular level, is due to different distances of the electron transfer within two ferrocene families. The second rationale is based on the Marcus outer-sphere electron-transfer formalism and the rate decrease with increasing reaction driving force is attributed to the inverted Marcus region for the electron-rich pentamethylated ferrocenes.

4. Experimental

4.1. Reagents

Horseradish peroxidase ($R/Z = 3$) was obtained from Dia-M and used as received. Ferroceneacetic acid (**6**) and 1,1′-ferrocenedicarboxylic acid (**12**) were purchased from Aldrich. Ferrocenyl methyl ketone oxime (**11**) was prepared as described [24,25]. Pentamethylferrocene derivatives (**15**–**17**) were synthesized using a recently reported procedure [26]. 1-Ferrocenylethanol (**10**) was obtained by reduction of acetylferrocene by $LiAlH_4$ [27]. 1,2,4,1′,2′,4′-Hexamethylferrocene (**18**) was a gift from Dr S.A. Yanovsky. 3-Ferrocenyl-3-oxobutyric (**8**) and 4-ferrocenyl-4-oxopentanoic (**9**) acids were obtained by treating ferrocene with the corresponding cyclic anhydride in the presence of $AlCl_3$ as described elsewhere [28]. 1-Et-1′-$(CO(CH_2)_2COOH)$Fc (**13**) and 1-*n*-Bu-1′-HOOCFc (**14**) were kindly provided by Dr B. Gautheron [29]. Triton X-100 was a Serva reagent. Hydrogen peroxide, buffer components, and other chemicals used were all Reakhim reagents of the highest purity available. The extinction coefficients for ferricenium cations formed in reaction (1) and listed in Table 3 were determined as described in detail elsewhere [8].

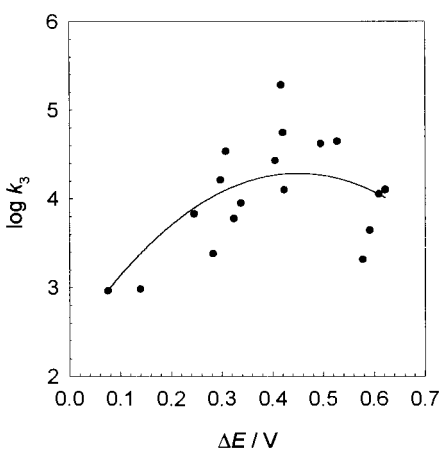

Fig. 6. Treatment of the kinetic data shown in Fig. 4 in terms of Eq. (5).

Table 3
Spectral characteristics of ferricenium cations derived from ferrocenes listed in Chart 1 (pH 7.0, phosphate 0.01 M)

No.	Ferrocene derivative	λ_{max} (nm)	ε (M^{-1} cm^{-1})
6	$FcCH_2COOH$	619	302 ± 8
8	$FcCO(CH_2)_2COOH$	439	450 ± 5
9	$FcCO(CH_2)_3COOH$	450	314 ± 9
10	FcCHOHMe	636	373 ± 2
11	FcC(Me)=NOH	704	245 ± 1
12	1,1′-$(HOOC)_2$Fc	638	53 ± 1
13	1-Et-1′-$(CO(CH_2)_2COOH)$ Fc	653	105 ± 2
14	1-n-Bu-1′-HOOCFc	638	323 ± 6
15	Cp*FeCp	742	285 ± 9
16	Cp*FeC_5H_4COOH	742	440 ± 6
17	Cp*$FeC_5H_4CH_2NMe_2$	747	203 ± 3
18	1,2,4,1′,2′,4′-Me_6Fc	738	282 ± 4

4.2. Kinetic and electrochemical measurements

All kinetic measurements were carried out on a Shimadzu UV-160A spectrophotometer equipped with a CPS-240A cell positioner/temperature controller. The solutions for kinetic runs were prepared as described in detail previously [9]. In some cases, poorly water-soluble ferrocenes were first dissolved in a minimal amount of ethanol and the resulting solution was then mixed with the phosphate buffer containing the requested amount of Triton X-100. The total amount of EtOH in the resulting reaction mixture never exceeded 1% by volume. The reactions were initiated by addition of 10 μl of the HRP solution (2.05×10^{-5} M) to the reaction mixture containing 1.0 ml of ferrocene solution (2.5×10^{-3} M), 30 μl of H_2O_2 solution (0.013 M), and 970 μl of 0.1 M phosphate buffer in a 1 cm quartz cell. The development of absorbance at the wavelength of maximum for a particular ferricenium cation was monitored until ca. 60% of the total amount of ferrocene was

oxidized. Practically linear steady-state portions at kinetic curves were observed up to 55% conversion and the corresponding slopes of absorbance versus time plots were taken as steady-state rates. Every kinetic parameter reported is a mean value of at least three determinations.

Cyclic voltammograms were obtained on a PC-interfaced potentiostat-galvanostat IPC-3 (Institute of Physical Chemistry, Russian Academy of Sciences, Moscow, Russia). A three-electrode scheme was used with working pyrolytic graphite electrode, saturated calomel reference electrode (SCE), and auxiliary Pt electrode. Unless otherwise indicated, all potentials reported in this paper are given against SCE.

Acknowledgements

The research described in this publication was made possible in part by financial support from the Russian Foundation for Fundamental Research (96-03-34328a, 99-03-070a). We are grateful to Dr B. Gautheron for providing ferrocene samples. V.N.G. thanks the Robert Havemann Foundation for the scholarship.

References

[1] A.D. Ryabov, Angew. Chem. Int. Ed. Engl. 30 (1991) 931.
[2] G. Jaouen, A. Vessières, I.S. Butler, Acc. Chem. Res. 26 (1993) 361.
[3] A.D. Ryabov, Ross. Khim. Zh. (1995) 139.
[4] J. Everse, K.E. Everse, M.B. Grisham (Eds.), Peroxidases in Chemistry and Biology, vols. I and II, CRC Press, Boca Raton, FL, 1991.
[5] P.R. Ortiz de Montellano, Ann. Rev. Pharmacol. Toxicol. 32 (1991) 90.
[6] M. Gajhede, D.J. Schuller, A. Henriksen, A.T. Smith, T.L. Poulos, Nat. Struct. Biol. 4 (1997) 1032.
[7] A. Henriksen, D.J. Schuller, K. Meno, K. Welinder, A.T. Smith, M. Gajhede, Biochemistry 37 (1998) 8054.
[8] V.N. Goral, M.I. Nelen', A.D. Ryabov, Anal. Lett. 28 (1995) 2139.
[9] A.D. Ryabov, V.N. Goral, J. Biol. Inorg. Chem. 2 (1997) 182.
[10] V.N. Goral, A.D. Ryabov, Biochem. Mol. Biol. Int. 45 (1998) 61.
[11] A.D. Ryabov, Y.N. Firsova, V.N. Goral, E.S. Ryabova, A.N. Shevelkova, L.L. Troitskaya, T.V. Demeschik, V.I. Sokolov, Chem. Eur. J. 4 (1998) 806.
[12] A.D. Ryabov, V.S. Kurova, V.N. Goral, M.D. Reshetova, J. Razumiene, R. Simkus, V. Laurinavičius, Chem. Mater. 11 (1999) 600.
[13] A.D. Ryabov, V.N. Goral, L. Gorton, E. Csöregi, Chem. Eur. J. 5 (1999) 961.
[14] R.A. Marcus, N. Sutin, Biochim. Biophys. Acta 811 (1985) 265.
[15] R.A. Marcus, Angew. Chem. Int. Ed. Engl. 32 (1993) 1111.
[16] R. Epton, M.E. Hobson, G. Marr, J. Organomet. Chem. 149 (1978) 231.
[17] I.V. Berezin, A.K. Yatsimirsky, K. Martinek, Usp. Khim. 42 (1973) 1729.
[18] K. Martinek, A.K. Yatsimirsky, A.V. Levashov, I.V. Berezin, in: K.L. Mittal (Ed.), Micellization, Solubilization, and Microemulsions, vol. 2, Plenum, New York, 1977, pp. 489.
[19] A.D. Ryabov, A. Amon, R.K. Gorbatova, E.S. Ryabova, B.B. Gnedenko, J. Phys. Chem. 99 (1995) 14072.
[20] H. Gray, J.R. Winkler, Ann. Rev. Biochem. 65 (1996) 537.
[21] L.K. Folkes, L.P. Candeias, FEBS Lett. 412 (1997) 305.
[22] L.P. Candeias, L.K. Folkes, P. Wardman, Biochemistry 36 (1997) 7081.
[23] Z.S. Farhangrazi, M.E. Fosset, L.S. Powers, W.R. Ellins, Biochemistry 34 (1995) 2866.
[24] E. Beckman, Chem. Ber. 23 (1890) 1680.
[25] E. Beckman, Liebigs Ann. Chem. 365 (1909) 200.
[26] B. Bildstein, A. Hradsky, H. Kopacka, R. Malleier, K.-H. Ongania, J. Organomet. Chem. 540 (1997) 127.
[27] F.S. Arimoto, A.C.J. Haven, J. Am. Chem. Soc. 77 (1955) 6295.
[28] K.L.J. Rinehart, R.J.J. Curby, P.L. Sokol, J. Am. Chem. Soc. 79 (1957) 3420.
[29] J. Tirouflet, R. Dabard, B. Gautheron, Compt. Rend. 256 (1963) 433.